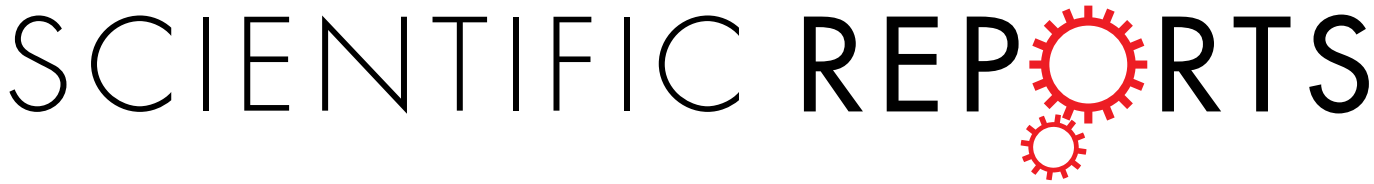

OPEN

A simple optimization approach for improving target dose homogeneity in intensity-modulated radiotherapy for sinonasal cancer

Received: 26 June 2015
Accepted: 25 September 2015
Published: 26 October 2015

Jia-Yang Lu[1,*], Ji-Yong Zhang[1,*], Mei Li[1,*], Michael Lok-Man Cheung[2,*], Yang-Kang Li[3,*], Jing Zheng[4,*], Bao-Tian Huang[1] & Wu-Zhe Zhang[1]

Homogeneous target dose distribution in intensity-modulated radiotherapy (IMRT) for sinonasal cancer (SNC) is challenging to achieve. To solve this problem, we established and evaluated a basal-dose-compensation (BDC) optimization approach, in which the treatment plan is further optimized based on the initial plans. Generally acceptable initial IMRT plans for thirteen patients were created and further optimized individually by (1) the BDC approach and (2) a local-dose-control (LDC) approach, in which the initial plan is further optimized by addressing hot and cold spots. We compared the plan qualities, total planning time and monitor units (MUs) among the initial, BDC, LDC IMRT plans and volumetric modulated arc therapy (VMAT) plans. The BDC approach provided significantly superior dose homogeneity/conformity by 23%–48%/6%–9% compared with both the initial and LDC IMRT plans, as well as reduced doses to the organs at risk (OARs) by up to 18%, with acceptable MU numbers. Compared with VMAT, BDC IMRT yielded superior homogeneity, inferior conformity and comparable overall OAR sparing. The planning of BDC, LDC IMRT and VMAT required 30, 59 and 58 minutes on average, respectively. Our results indicated that the BDC optimization approach can achieve significantly better dose distributions with shorter planning time in the IMRT for SNC.

Malignancies of the nasal cavity and paranasal sinuses (sinonasal cancer, SNC) are relatively rare and usually presented with locally advanced disease by the time of diagnosis[1–3]. Surgical resection combined with postoperative radiotherapy can improve the locoregional control and overall survival rates[4,5]. Conventional radiotherapy often leads to radiation-induced blindness, retinopathy and optic neuropathy by up to 37%, 40% and 47% of patients, respectively owing to the special anatomy with close proximity of several critical structures such as lenses, eyes, optic nerves, optic chiasm and brainstem[6]. Several reports have demonstrated that intensity-modulated radiotherapy (IMRT) for SNC resulted in significantly reduced ocular toxicity and other side effects while maintaining disease control and survival at least[6–8].

However, the IMRT planning for SNC is challenging. Besides the close proximity to the nearby critical structures, the presence of the dose inhomogeneity in this particular site also complicates the treatment

[1]Department of Radiation Oncology, Cancer Hospital of Shantou University Medical College, Shantou 515000, Guangdong, China. [2]Department of Clinical Oncology, Prince of Wales Hospital, Shatin, Hong Kong 999077, China. [3]Department of Radiology, Cancer Hospital of Shantou University Medical College, Shantou 515000, Guangdong, China. [4]Department of Laboratory, Shantou Central Hospital, Affiliated Shantou Hospital of Sun Yat-sen University, Shantou 515000, Guangdong, China. *These authors contributed equally to this work. Correspondence and requests for materials should be addressed to B.-T.H. (email: tianjia2025@163.com)

Case	Gender	Age (years)	Tumor site	Aim of radiotherapy	Pathological type	Stage
1	Male	65	nasal cavity	Postopereative	Melanoma	T3N0M0
2	Male	63	nasal cavity	Postopereative	Melanoma	T2N0M0
3	Male	32	nasal cavity	Postopereative	Esthesioneuroblastoma	T3N0M0
4	Female	61	nasal cavity	Definitive	NK/T cell lymphoma	T3N0M0
5	Male	59	maxillary sinus	Postopereative	Sarcoma	T2N0M0
6	Female	51	nasal cavity	Definitive	NK/T cell lymphoma	T3N0M0
7	Female	65	nasal cavity	Definitive	NK/T cell lymphoma	T3N0M0
8	Male	62	maxillary sinus	Postopereative	SCC	T4N0M0
9	Female	53	nasal cavity	Postopereative	SCC	T4N0M0
10	Female	64	nasal cavity	Postopereative	Esthesioneuroblastoma	T2N0M0
11	Male	50	ethmoid sinus	Postopereative	SCC	T4N0M0
12	Male	65	maxillary sinus	Postopereative	Adenoid cystic carcinoma	T3N0M0
13	Female	51	nasal cavity	Postopereative	Melanoma	T4N0M0

Table 1. Patient characteristics. *Abbreviations:* NK = Natural killer; SCC = Squamous cell carcinoma.

Structure	Planning constraint(s)
PTV	$D_{95\%} = 60$ Gy
	$D_{2\%} < 66$ Gy (110% of the prescription dose)
Lens	$D_{2\%} < 10$ Gy
Optic nerve	$D_{2\%} < 54$ Gy
Optic chiasm	$D_{2\%} < 54$ Gy
Eye	$D_{2\%} < 50$ Gy
Spinal cord	$D_{2\%} < 40$ Gy
Brainstem	$D_{2\%} < 50$ Gy
Temporal lobe	$D_{2\%} < 60$ Gy
Cochlea	$D_{5\%} < 55$ Gy; $D_{mean} < 45$ Gy
Pituitary	$D_{2\%} < 64$ Gy
Oral cavity	$D_{mean} < 30$ Gy
Parotid	$D_{50\%} < 30$ Gy; $D_{mean} < 26$ Gy
Normal tissue	As low as possible

Table 2. Planning goals for the treatment plans for sinonasal cancer. *Abbreviation:* PTV = planning target volume; $D_{x\%}$ = dose that is reached or exceeded in x% of the volume; D_{mean} = mean dose.

planning[9]. The target volume typically contains large volumes of air cavities and the buildup region, in which the optimization-convergence error (OCE)[10,11] is extraordinarily significant. The OCE can result in dose discrepancy between the optimizer plans and the finally-calculated plans thus leading to locally high doses (hot spots) or locally low doses (cold spots). The OCE is a systematic error which originates from several major sources including tissue heterogeneity, the buildup region, multi-leaf collimator (MLC) modulation and the optimization algorithm, as described by Dogan *et al.*[11]. The OCE is not able to be overcome by designing optimal arrangement and number of beams, by which IMRT plans are usually effectively improved[12,13].

In this study, we proposed an optimization approach referred to as basal dose compensation (BDC), in which an initial IMRT plan was utilized as a base dose plan for compensating for the OCE. We applied it to SNC cases and then evaluated it by comparing with the initial plan and another commonly-used optimization approach named local dose control (LDC)[14,15]. Moreover, volumetric modulated arc therapy (VMAT) technique, an advanced IMRT format with continually rotational gantry, which was previously reported to be dosimetrically superior[16] or comparable[9] to conventional IMRT technique in SNC cases, was also adopted for further comparison in this study.

						P value (BDC IMRT *vs*)		
		Initial IMRT	BDC IMRT	LDC IMRT	VMAT	Initial IMRT	LDC IMRT	VMAT
PTV	$D_{2\%}$ (Gy)	65.56 ± 1.11	62.84 ± 0.74	63.64 ± 0.73	63.52 ± 0.79	0.001	0.001	0.001
	$D_{98\%}$ (Gy)	58.63 ± 0.62	59.36 ± 0.25	59.03 ± 0.48	58.98 ± 0.30	0.002	0.060	0.001
	$D_{50\%}$ (Gy)	62.31 ± 0.65	61.23 ± 0.29	61.73 ± 0.37	61.87 ± 0.50	0.001	0.001	0.001
	HI	0.111 ± 0.024	0.057 ± 0.015	0.075 ± 0.015	0.073 ± 0.017	0.001	0.002	0.001
	CI	0.795 ± 0.033	0.866 ± 0.016	0.822 ± 0.023	0.895 ± 0.017	0.001	0.001	0.002
CL lens	$D_{2\%}$ (Gy)	6.77 ± 1.22	6.74 ± 1.28	8.28 ± 1.73	7.88 ± 0.83	0.594	0.001	0.004
IL lens	$D_{2\%}$ (Gy)	8.95 ± 2.11	8.93 ± 2.19	10.65 ± 3.80	8.79 ± 1.47	0.484	0.001	0.507
CL optic nerve	$D_{2\%}$ (Gy)	45.42 ± 9.77	43.97 ± 9.82	47.16 ± 12.63	49.28 ± 5.27	0.003	0.006	0.007
IL optic nerve	$D_{2\%}$ (Gy)	53.53 ± 3.49	52.00 ± 3.68	56.05 ± 4.77	53.47 ± 3.66	0.028	0.001	0.011
Optic chiasm	$D_{2\%}$ (Gy)	46.15 ± 7.00	45.57 ± 6.80	48.58 ± 9.75	44.40 ± 9.92	0.402	0.002	0.552
CL eye	$D_{2\%}$ (Gy)	35.55 ± 14.04	34.95 ± 13.96	36.49 ± 14.37	34.50 ± 9.16	0.030	0.001	0.807
IL eye	$D_{2\%}$ (Gy)	47.06 ± 4.92	46.04 ± 4.85	49.95 ± 5.44	44.84 ± 4.99	0.004	0.001	0.084
Spinal cord	$D_{2\%}$ (Gy)	15.80 ± 5.99	15.46 ± 5.81	15.71 ± 585	10.46 ± 7.17	0.025	0.249	0.002
Brainstem	$D_{2\%}$ (Gy)	38.33 ± 4.77	38.24 ± 4.91	38.58 ± 4.92	29.91 ± 8.45	0.861	0.043	0.002
CL temporal lobe	$D_{2\%}$ (Gy)	38.88 ± 10.89	37.50 ± 9.62	37.71 ± 13.32	39.25 ± 8.33	0.019	0.064	0.196
IL temporal lobe	$D_{2\%}$ (Gy)	50.67 ± 6.40	49.98 ± 6.13	48.46 ± 13.48	45.50 ± 6.74	0.016	0.116	0.001
CL cochlea	$D_{5\%}$ (Gy)	24.61 ± 14.92	24.55 ± 14.90	25.42 ± 15.58	28.76 ± 8.64	0.286	0.002	0.152
	D_{mean} (Gy)	19.06 ± 11.36	18.98 ± 11.25	19.60 ± 11.81	25.74 ± 6.82	0.249	0.002	0.011
IL cochlea	$D_{5\%}$ (Gy)	35.10 ± 9.23	34.18 ± 8.80	35.89 ± 9.50	33.43 ± 8.36	0.013	0.003	0.600
	D_{mean} (Gy)	28.31 ± 7.15	27.71 ± 7.29	28.76 ± 7.82	29.35 ± 6.30	0.007	0.004	0.382
Pituitary	$D_{2\%}$ (Gy)	44.38 ± 9.33	44.44 ± 9.48	45.34 ± 10.45	41.26 ± 12.19	0.861	0.075	0.087
Oral cavity	$D_{50\%}$ (Gy)	16.84 ± 7.07	16.58 ± 6.95	17.25 ± 7.20	8.26 ± 8.70	0.030	0.003	0.004
	D_{mean} (Gy)	22.65 ± 6.24	22.25 ± 6.03	22.84 ± 6.29	16.85 ± 6.45	0.002	0.002	0.001
CL parotid	$D_{50\%}$ (Gy)	5.55 ± 6.76	5.33 ± 6.56	5.42 ± 6.51	7.45 ± 7.09	0.002	0.028	0.003
	D_{mean} (Gy)	6.64 ± 5.20	6.39 ± 5.08	6.56 ± 5.10	9.15 ± 5.44	0.001	0.001	0.002
IL parotid	$D_{50\%}$ (Gy)	8.48 ± 6.57	8.00 ± 6.36	8.26 ± 6.51	8.98 ± 7.30	0.001	0.003	0.650
	D_{mean} (Gy)	9.55 ± 6.10	9.07 ± 5.91	9.35 ± 6.06	11.00 ± 6.47	0.001	0.001	0.004
Normal tissue	$D_{50\%}$ (Gy)	2.82 ± 2.22	2.71 ± 2.14	2.83 ± 2.22	1.37 ± 1.24	0.001	0.001	0.001
	D_{mean} (Gy)	7.49 ± 2.08	7.30 ± 2.02	7.47 ± 2.08	6.90 ± 1.94	0.001	0.001	0.004
Monitor units		862 ± 109	958 ± 152	1157 ± 320	410 ± 19	0.001	0.006	0.001
Planning time	(minute)	NA	30.3 ± 4.3	58.6 ± 23.6	57.6 ± 6.7	NA	0.001	0.001

Table 3. Dosimetric parameters for the initial, basal-dose-compensation (BDC), local-dose-control (LDC) intensity-modulated radiotherapy (IMRT) plans and volumetric modulated arc therapy (VMAT) plans. *Abbreviations:* PTV = planning target volume; CL = contalateral; IL = ipsilateral; NA = not applicable; $D_{x\%}$ = dose which is reached or exceeded in x% of the volume; HI = homogeneity index; CI = conformity index; D_{mean} = mean dose.

Methods

Ethics Statement. The protocol was approved by the Ethical Commission of the Cancer Hospital of Shantou University Medical College. Because this was not a treatment-based study, our institutional review board waived the need for written informed consent from the participants. The patient information was anonymized and de-identified to protect patient confidentiality. The methods were carried out in accordance with the approved guidelines.

Patient characteristics. We retrospectively identified thirteen patients with malignancies of the nasal cavity, maxillary sinus and ethmoid sinus with stages T2–T4, N0 and M0, according to the American Joint Committee on Cancer (AJCC) 2010 7th edition staging criteria. Of the thirteen patients, seven were males and the remaining six were females, with the median age of 61 years (range, 32–65 years). The pathological types and other detailed information are listed in Table 1.

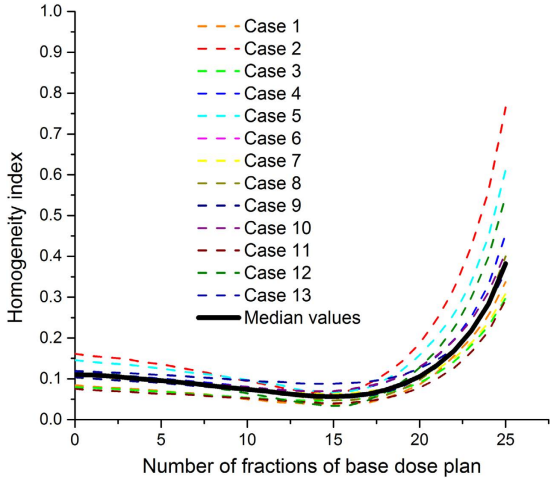

Figure 1. Variation of homogeneity index (HI) under the impact of the number of fractions of base dose plan (NOF_BDP) in the basal-dose-compensation (BDC) optimization approach.

CT simulation, target and organ-at-risk (OAR) delineation. The patient immobilization was performed using custom-made thermoplastic masks in the supine position. CT datasets with 3-mm slice thickness were acquired using the 16-slice Big Bore Brilliance CT scanner (Philips Medical System Inc., Cleveland, OH). The CT images were subsequently transferred to the Eclipse version 10.0 (Varian Medical System, Palo Alto, CA) treatment planning system for contouring and treatment planning.

All target volumes were delineated by the attending radiation oncologists. Gross tumor volume (GTV) was defined as the visible extent of tumor identified using contrasted CT, MR and positron emission tomography (PET). Clinical target volume (CTV) comprises the primary tumor bed and the zones at risk of harboring microscopic extension. To account for setup errors, potential intrafractional shifts of patients and mechanical inaccuracies, 0.5 cm margins were added to the CTV to form the planning target volume (PTV). The PTV was prescribed a 60-Gy dose (2 Gy/fraction) administered in 30 fractions. The median volume of the PTV was 183 cubic centimeters (cc) with the range of 102–259 cc.

OARs were contoured including the lenses, optic nerves, optic chiasm, eyes, spinal cord, brainstem, temporal lobes, cochleae, pituitary, oral cavity, parotids. The surrounding normal tissue was defined as the body minus the PTV.

IMRT and VMAT planning. Seven sliding-window fields of 6-MV photons from a TrueBeam (Varian Medical Systems, Palo Alto, USA) linear accelerator were generated for each IMRT plan in Eclipse. Five coplanar fields were set at 260°, 330°, 0°, 30° and 100° gantry angles and two non-coplanar fields were set at 30° and 330° gantry angles with a couch rotation of 90°. The beam arrangement setting was based on the study by Jeong *et al.*[16], except that the collimator angles of the coplanar fields with gantry angles of 30° and 330° were optimized for each case aiming at shielding the lenses. For each VMAT plan, two coplanar full arcs were adopted[17] and the collimator angles were set to 30° and 330°, respectively to minimize the tongue-and-groove effect. The IMRT and VMAT optimizations were performed using the Dose Volume Optimizer (DVO version 10.0.28) and Progressive Resolution Optimizer (PRO version 10.0.28) algorithms, respectively. The Anisotropic Analytical Algorithm (AAA, version 10.0.28) was applied for the final dose calculation. The final plans were normalized to insure that 95% of the PTV received the prescribed dose.

According to the International Commission on Radiation Units and Measurements (ICRU) report 83[18], the notation D_x represents the dose that was reached or exceeded in x of the volume. $D_{2\%}$ and $D_{98\%}$ indicate the near-maximum and near-minimum doses, respectively. In the inverse optimization objectives, the PTV coverage were assigned the highest priorities, followed by the avoidance of overdosing the lenses, optic chiasm and optic nerves, to preserve mono-lateral vision at least[19], and the other OAR sparing was given the last priority. The planning goals are shown in Table 2.

The planning objectives from a template were applied and adjusted to generate a generally acceptable initial IMRT plan. In the BDC optimization approach, the number of fractions (NOF) of the initial IMRT plan was modified to x% ($0 \leq x < 100$) of the total prescribed NOF to generate a "base dose plan" with x% of the total prescribed dose. Then, the base dose plan was duplicated to create a "top dose plan" with (100–x)% of the total prescribed NOF. Afterwards, the top dose plan was further optimized based on the base dose plan using the "base dose plan" function of Eclipse, while maintaining the optimization objectives unmodified. The "base dose plan" function of Eclipse enabled the system to optimize a plan (as top dose plan) while taking another plan (as base dose plan) into account, aiming to achieve an optimal plan sum by making up for inadequacies (hot/cold spots) in the base dose plan. At this point,

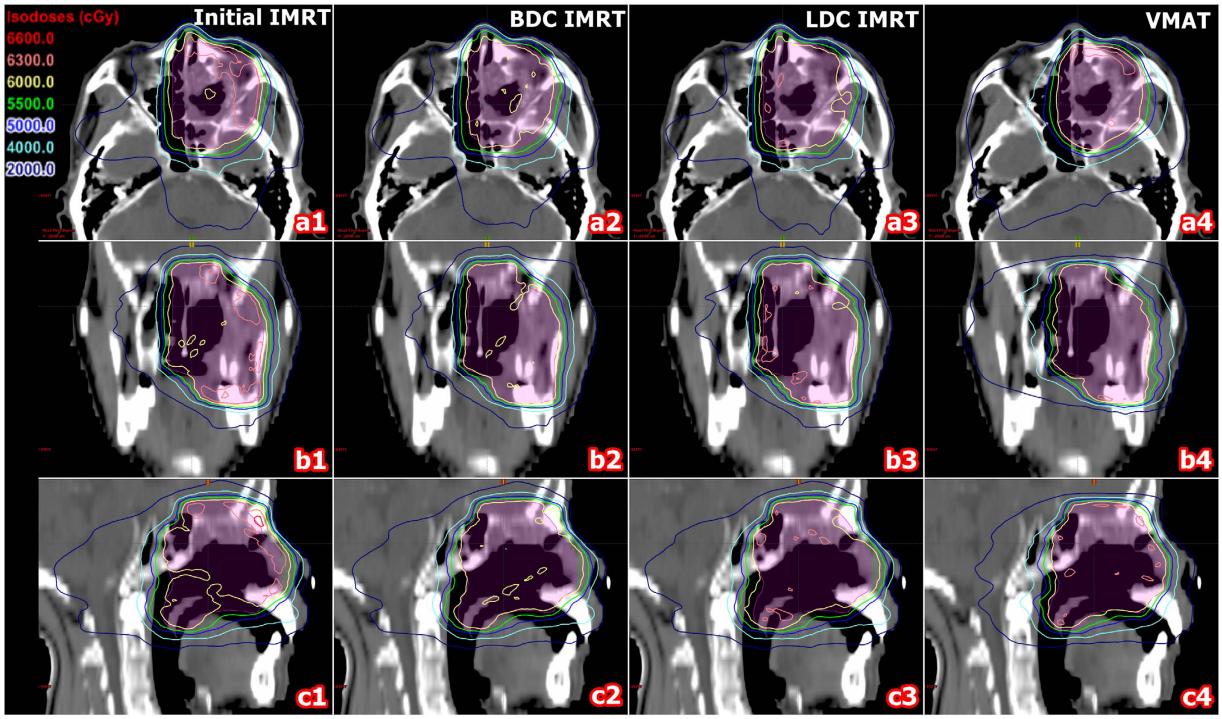

Figure 2. Dose distributions of the initial (a1,b1,c1), basal-dose-compensation (BDC) (a2,b2,c2), local-dose-control (LDC) (a3,b3,c3) intensity-modulated radiotherapy (IMRT) plans and volumetric modulated arc therapy (VMAT) (a4,b4,c4) plans for one representative case.

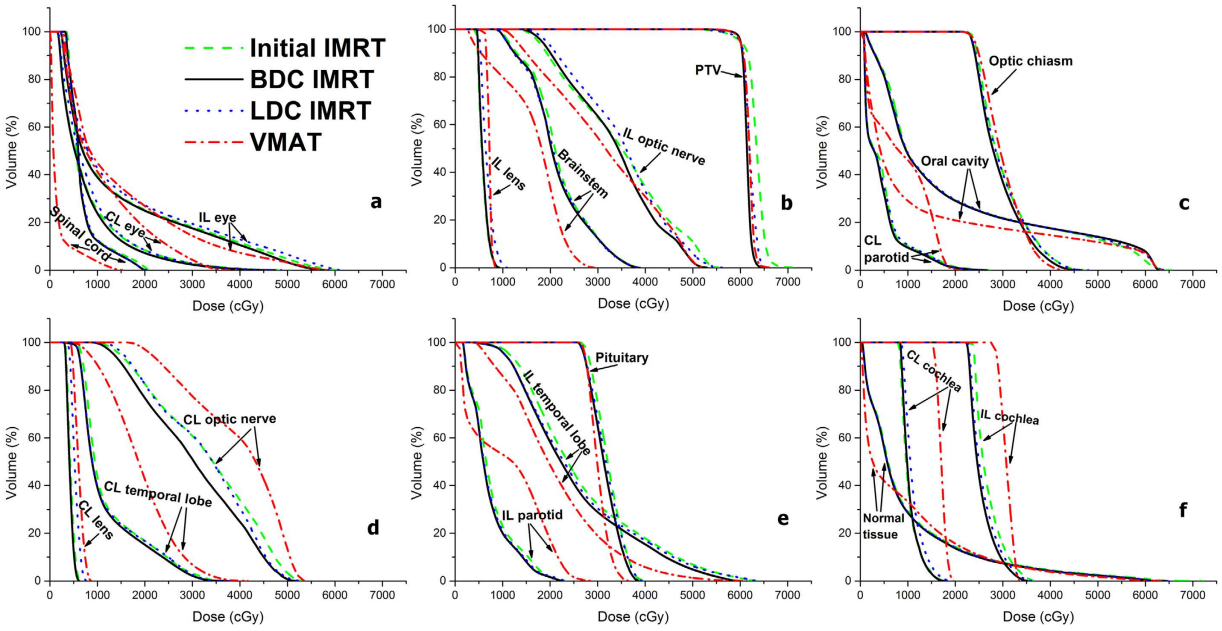

Figure 3. Dose-volume histograms (DVHs) of the initial, basal-dose-compensation (BDC), local-dose-control (LDC) intensity-modulated radiotherapy (IMRT) plans and volumetric modulated arc therapy (VMAT) plans for one representative case. The charts show the DVHs for spinal cord, contralateral (CL) eye, ipsilateral (IL) eye (**a**), IL lens, brainstem, IL optic nerve, planning target volume (PTV) (**b**), CL parotid, oral cavity, optic chiasm (**c**), CL lens, CL temporal lobe, CL optic nerve (**d**), IL parotid, IL temporal lobe, pituitary (**e**), normal tissue, CL cochlea and IL cochlea (**f**).

the prescribed dose of the plan sum (the base dose plan plus the top dose plan) was equivalent to the original prescription dose. After calculating the final dose of the top dose plan, the NOF of top dose plan (NOF_TDP) was restored from (100–x)% to 100% of the prescribed NOF. The top dose plan with 100% of the prescribed NOF was the final treatment plan for delivery. To establish the BDC approach for SNC cases, we needed to identify the optimal value of the x% of the prescribed NOF of base dose plan (NOF_BDP). Our pilot experiment demonstrated that the dose homogeneity became extremely poor when the NOF_BDP was > 25. Therefore, we tested different NOF_BDP, from 1 to 25 in the present study, to find out which was the best NOF_BDP when applying the BDC approach to SNC cases (the corresponding NOF_TDP was equal to 30 minus NOF_BDP). Using the established BDC approach, the initial IMRT plans were improved by further optimization and the final IMRT plans were named BDC IMRT plans.

In the LDC approach[14,15], the initial optimization objects were kept unchanged, and the cold-spot ($\leq$ 100% of prescribed dose, within PTV) and hot-spot ($\geq$110%, 107% or 105% of the prescribed dose) regions were converted into dose-controlling structures and were then assigned additional lower objectives (101–105% of the prescribed dose) and upper objectives (88%–99% of the prescribed dose), respectively for the further optimization processes. When the final plans achieved the planning goals, the LDC IMRT plans were completed.

The VMAT plans were optimized based on the objectives applied in the initial IMRT plans and were further optimized until the clinically acceptable plans were achieved.

A distributed calculation framework (DCF) was adopted to accelerate the final dose calculation. The total treatment planning time, which accounted for the initial planning time, was recorded for the BDC, LDC IMRT and VMAT plans.

Plan evaluation. According to the ICRU report 83, the homogeneity index (HI), as a measure of the PTV dose homogeneity, was calculated using the following formula ($D_{50\%}$ indicates the median dose):

$$HI = \frac{D_{2\%} - D_{98\%}}{D_{50\%}} \tag{1}$$

A conformity index (CI)[20] which takes into consideration the overlap between target volume (TV) and prescription isodose volume (PIV), was used to measure the target dose conformity and was computed using the formula below:

$$CI = \frac{(TV\ within\ PIV)^2}{TV \times PIV} \tag{2}$$

An HI value of 0 stands for the ideal homogeneity, and a CI value of 1 stands for the ideal conformity. $D_{2\%}$ was used for evaluating the hot spot, and $D_{98\%}$ was used for evaluating the cold spot. The monitor units (MUs) per fraction were also appraised for all plans.

Statistical analysis. To determine the differences between BDC and initial IMRT, the differences between BDC and LDC IMRT, and the differences between BDC IMRT and VMAT, two-sided paired Wilcoxon signed rank test was used. Data analysis was performed using the SPSS version 19 software (SPSS, Inc., Chicago, IL, USA). Differences were considered to be statistically significant when *P*-value was < 0.05.

Results

Establishment of the BDC approach and the HI variation. The NOF_BDP indicated the degree of compensation. The HI value of the BDC IMRT plans (optimized top dose plans with 100% of the prescribed NOF) was closely related to the NOF_BDP in the BDC approach. In each case, the NOF_BDP resulting in the lowest HI (indicating the best dose homogeneity) was considered to be the best NOF_BDP. Since the variation tendencies of HIs with the change of NOF_BDP were similar in all cases (see Fig. 1), the frequently-observed best NOF_BDP corresponding to the lowest HI in the greatest number of cases, should be the best one for general use purpose. In our study, the best NOF_BDP values were 15 in 9 cases and 14 in 4 cases, so the 15 (50% of the total prescribed NOF) was determined as the best NOF_BDP for general use in SNC cases.

When the NOF_BDP was 0 (corresponding NOF_TDP was 30), no base dose plan was used for compensation, and the HI value of the BDC IMRT plan was equivalent to that of the initial IMRT plan undoubtedly; the HI decreased slightly (lower HI value indicates better dose homogeneity) approaching the lowest value when the NOF_BDP increased towards approximately 15; when the NOF_BDP was more than approximately 15 and continued to increase towards the prescribed NOF (the NOF_TDP was less than approximately 15 and continued to decrease), the HI increased faster and faster towards the positive infinity, indicating that the dose homogeneity became worse and worse.

In general, the HI was sensitive to the choice of NOF_BDP. When the NOF_BDP value was selected between 14 and 16, low sensitivity with only $< 3\%$ difference from the lowest HI was observed; when the NOF_BDP value was between 0 and 13, median sensitivity with 8%–96% difference from the lowest

HI was observed; when the NOF_BDP value was between 17 and 25, high sensitivity with 12%–579% difference was observed.

Target dose homogeneity and conformity. Table 3 presents the PTV dose-volume parameters for the four plans. The BDC IMRT provided the best homogeneity and satisfactory conformity. With regards to the HI, BDC IMRT was significantly better than initial, LDC IMRT and VMAT by $48.2\% \pm 11.8\%$, $23.3\% \pm 16.1\%$ and $23.0\% \pm 9.1\%$, respectively. With regards to the hot and cold spots, BDC IMRT provided lower $D_{2\%}$ values by approximately 1.1%–4.1% and higher $D_{98\%}$ values by 0.6%–1.3%. Significantly fewer hot spots of $\geq$ 105% (63 Gy) of the prescribed dose for the PTV were shown in the isodose distributions for BDC IMRT (Fig. 2), which also had a steeper dose-volume histogram (DVH) curve of the PTV (Fig. 3). In terms of the CI, BDC IMRT were superior to initial, LDC IMRT by $9.2\% \pm 3.9\%$ and $5.5\% \pm 2.4\%$, respectively, but inferior to VMAT by $3.2\% \pm 1.9\%$.

OAR sparing. Table 3 summarizes the dose-volume parameters of OARs for the four plans. Compared with the initial and LDC IMRT, the BDC IMRT tended to deposit slightly lower doses to the OARs, and most of the *P* values were < 0.05. BDC IMRT reduced $D_{2\%}$ to the bilateral optic nerves and eyes, by approximately 1.7%–3.4% compared with initial IMRT and by 4.4%–7.7% compared with LDC IMRT. Besides, BDC IMRT had similar $D_{2\%}$ to the bilateral lenses and optic chiasm compared with initial IMRT, whereas BDC IMRT demonstrated lower $D_{2\%}$ to the contralateral lens, ipsilateral lens and optic chiasm by 17.7%, 13.5% and 5.2%, respectively compared with LDC IMRT. Concerning the bilateral temporal lobes, BDC IMRT yielded 1.3%–3.0% lower $D_{2\%}$ than initial IMRT, and were comparable to LDC IMRT. In addition, BDC IMRT delivered lower doses to the cochleae by up to 4.6%, and also delivered lower doses to the oral cavity, parotids and normal tissue by 1.7%–6.7%.

When compared with VMAT, BDC IMRT allowed significant reductions of the $D_{2\%}$ to the contralateral lens, contralateral- and ipsilateral optic nerve by 14.8%, 11.5% and 2.7%, respectively, and significant reductions of the D_{mean} to the contralateral cochlea, $D_{50\%}$ and D_{mean} of the contralateral parotid and D_{mean} to the ipsilateral parotid by 29.4%, 30.2%, 31.5% and 13.1%, respectively. However, BDC IMRT gave higher $D_{2\%}$ values to the spinal cord, brainstem and ipsilateral temporal lobe by 100.3%, 34.7% and 10.3%, respectively, and higher $D_{50\%}$ and D_{mean} to the oral cavity, higher $D_{50\%}$ and D_{mean} of the normal tissue, by 177%, 37.3%, 123.3% and 6.1%, respectively. With regards to the doses to the ipsilateral lens, optic chiasm, bilateral eyes, contralateral temporal lobe, pituitary, ipsilateral cochlea and the $D_{5\%}$ to the contralateral cochlea as well as the $D_{50\%}$ to the ipsilateral parotid, no statistically significant differences were observed between BDC IMRT and VMAT.

Planning time and MUs. The average planning time of BDC IMRT was 30.3 minutes, which was less than those of LDC IMRT and VMAT by 41.9% and 46.5%, respectively. The MUs of BDC IMRT were higher than those of initial IMRT and VMAT by 10.7% and 134.6%, respectively, but were lower than those of LDC IMRT by 14.2%.

Discussion

The achievement of uniform dose distribution of PTV and the sparing of the nearby critical structures, especially the optic structures, were challenging in SNC cases even treated with IMRT. In this study, a BDC optimization approach was well established, and its dosimetric characteristics were evaluated. We found that this approach could substantially improve the dose homogeneity of the target, while improving the target conformity and OAR sparing, thus it may increase the therapeutic ratio for SNC patients. Additionally, this approach could achieve comparable overall results to the VMAT delivery technique.

The improvement of HI by approximately 23%–48% with the established BDC approach may have a potential clinical benefit for SNC patients. Underdosage within the target volume may lead to the likelihood of tumor recurrence. Overdosage within or out of the target volume, may lead to severe acute reactions or late complications, because the target volume of SNC typically contains such tissues as the mucosa, submucosa, nerves and bone[21]. Thus, the improvement of homogeneity may reduce the risk of tumor recurrence and reduce the unnecessary radiation-induced toxicity caused by hot-spot dose.

Moreover, the BDC approach demonstrated improvements with respect to the target conformity and OAR sparing. The BDC approach can reduce the doses delivered to the lenses, optic nerves and chiasm as well as eyes by up to 18%. Although Duprez *et al.*[6] have reported that the IMRT technique could minimize ocular toxicity, such as blindness and optic neuropathy, compared with conventional radiotherapy technique, there were still 10 cases of late Grade 3 tearing and 1 case of late Grade 3 visual impairment in 86 patients available for late toxicity evaluation. Therefore it is necessary to develop the IMRT technique to further minimize the dose delivered to the optic pathways. Besides, Bhandare *et al.*[22] observed that the sensorineural hearing loss is significantly correlated with dose to cochlea, and our data showed that the BDC approach can reduce the dose to cochlea by up to 5% and may thus reduce the risk of sensorineural hearing loss. Moreover, the BDC approach can reduce the doses to the temporal lobes, oral cavity and parotids in varying degrees, so it may have the potential to lower the risks of temporal lobe injury[23], oral mucositis[24] and xerostomia[25,26].

Another superiority of the BDC optimization approach lies in its shorter planning time. The explanation is that an excellent homogeneous dose distribution can be effortlessly achieved via a single further

optimization and the required procedure of modifying one parameter (NOF_BDP) is very simple. Reduction of the planning time is beneficial for reducing the time that patients must wait until the start of treatment and thus for relieving patients' anxieties. By contrast, the LDC approach is time-consuming because multiple further optimizations are usually required, and additionally, the delineation of the dose-controlling structures and the assignment and adjustment of new dose objectives usually take a certain amount of time. On the other hand, the VMAT planning time is also longer compared to BDC IMRT because the calculating process of AAA and optimizing process of PRO is time-consuming. With the progress of algorithms, VMAT planning time would decrease in the future.

Although the defect of the BDC approach lies in the increasing of the MUs by 11% compared with the initial IMRT, the MUs were still lower than those of LDC IMRT. VMAT had the advantage of significantly lower MUs and normal-tissue dose. Considering the higher doses to normal tissue and the excessive MUs may increase the risk of radiation-induced secondary malignancies[27] in theory, the VMAT technique is superior in this situation.

Conventionally, planers employ the base dose function to optimize a second-course plan (as top dose plan), e.g., a boost plan, based on the first-course plan (as base dose plan), to achieve an optimal plan sum (top dose plan plus base dose plan) in the optimizer. However, in the BDC approach, the base dose function is used in a new way; here, it is adopted to achieve a homogeneous-dose plan (top dose plan) in the finally-calculated version instead of a plan sum in the optimizer. In principle, the base dose function is utilized to compensate for the OCE. If the OCE introduces a hot spot into the finally-calculated dose of the initial plan (base dose plan), the BDC plan (top dose plan) will generate a cold spot in the same region to obtain a homogeneous summed dose. After final dose calculation of the BDC plan (top dose plan), the OCE introduces a hot spot into the cold-spot region of the BDC plan (top dose plan), and as a result, the final BDC plan will achieve a uniform dose.

Numerous studies have focused on the possible approaches or techniques to solve the OCE. The LDC optimization method described by Süss *et al.*[14] and applied by Xhaferllari *et al.*[15] is helpful for overcoming the OCE, but only locally effective in the dose-controlling region. It is a "trial and error" approach because planners need to manually adjust the additional objectives. On the contrary, the BDC method is globally effective and is a systematic approach. According to the review by Broderick *et al.*[28] and other previous studies[29,30], the Direct Aperture Optimization (DAO) technique incorporates series of deliverable MLC shapes instead of ideal intensity maps in the optimizer and is therefore able to eliminate the error contributed by MLC modulation. Unfortunately, this technique is not available in non-DAO treatment planning systems, e.g., Eclipse version 10.0. Verbakel *et al.*[31] have reduced the error originating from tissue heterogeneity by separating the PTV into low- and relatively high-density regions and subsequently setting a higher dose goal for the low-density region in the optimizer. This method is effective in the lung cancer cases, but it is not effective enough for SNC cases. As tested in our pilot study, a clinically acceptable plan with $D_{2\%}$ of PTV $< 110\%$ of prescribed dose could not be achieved with this method. Zacarias and Mill[31] also utilized the base dose function to solve the OCE, but that method is not the same as ours, because it required a complicated process and software and thus resulted in increased planning steps and time. On the contrary, our approach is much simpler and practical for routine use.

The limitation of this study is that only the dosimetric characteristics of the BDC approach were reported. Whether this proposed approach can bring real benefits to SNC patients remains questionable. The actual clinical benefits should be proved by follow-up in our further studies.

Conclusion

In this study, we established and evaluated a simple optimization method referred to as basal-dose-compensation approach for SNC. We found that this approach can improve the target dose homogeneity, conformity and OAR sparing, with shorter planning time and with acceptable MU number. In addition, it can achieve comparable overall dosimetric results to VMAT. Consequently, the proposed optimization method is recommended for incorporation into routine clinical practice for the IMRT for SNC.

References

1. Muir, C. S. & Nectoux, J. Descriptive epidemiology of malignant neoplasms of nose, nasal cavities, middle ear and accessory sinuses. *Clin Otolaryngol Allied Sci.* **5,** 195–211 (1980).
2. Harbo, G. *et al.* Cancer of the nasal cavity and paranasal sinuses. A clinico-pathological study of 277 patients. *Acta Oncol.* **36,** 45–50 (1997).
3. Mahalingappa, Y. B. & Khalil, H. S. Sinonasal malignancy: presentation and outcomes. *J Laryngol Otol.* **128,** 654–657 (2014).
4. Meng, X. J. *et al.* Impact of different surgical and postoperative adjuvant treatment modalities on survival of sinonasal malignant melanoma. *BMC Cancer.* **14,** 608 (2014).
5. Hollen, T. R. *et al.* Esthesioneuroblastoma of the nasal cavity. *Am J Clin Oncol.* **38,** 311–314 (2015).
6. Duprez, F. *et al.* IMRT for sinonasal tumors minimizes severe late ocular toxicity and preserves disease control and survival. *Int J Radiat Oncol Biol Phys.* **83,** 252–259 (2012).
7. Dirix, P., Vanstraelen, B., Jorissen, M., Vander Poorten, V. & Nuyts, S. Intensity-modulated radiotherapy for sinonasal cancer: improved outcome compared to conventional radiotherapy. *Int J Radiat Oncol Biol Phys.* **78,** 998–1004 (2010).
8. Daly, M. E. *et al.* Intensity-modulated radiation therapy for malignancies of the nasal cavity and paranasal sinuses. *Int J Radiat Oncol Biol Phys.* **67,** 151–157 (2007).

9. Nguyen, K. *et al.* A dosimetric comparative study: volumetric modulated arc therapy vs intensity-modulated radiation therapy in the treatment of nasal cavity carcinomas. *Med Dosim.* **38,** 225–232 (2013).
10. Jeraj, R., Keall, P. J. & Siebers, J. V. The effect of dose calculation accuracy on inverse treatment planning. *Phys Med Biol.* **47,** 391–407 (2002).
11. Dogan, N. *et al.* Improving IMRT dose accuracy via deliverable Monte Carlo optimization for the treatment of head and neck cancer patients. *Med Phys.* **33,** 4033–4043 (2006).
12. Budrukkar, A. N., Hope, G., Cramb, J., Corry, J. & Peters, L. J. Dosimetric study of optimal beam number and arrangement for treatment of nasopharyngeal carcinoma with intensity-modulated radiation therapy. *Australas Radiol.* **48,** 45–50 (2004).
13. Cheng, M. C. *et al.* Optimal beam design on intensity-modulated radiation therapy with simultaneous integrated boost in nasopharyngeal cancer. *Med Dosim.* **39,** 246–250 (2014).
14. Suss, P., Bortz, M., Kufer, K. H. & Thieke, C. The critical spot eraser-a method to interactively control the correction of local hot and cold spots in IMRT planning. *Phys Med Biol.* **58,** 1855–1867 (2013).
15. Xhaferllari, I., Wong, E., Bzdusek, K., Lock, M. & Chen, J. Automated IMRT planning with regional optimization using planning scripts. *J Appl Clin Med Phys.* **14,** 4052 (2013).
16. Jeong, Y. *et al.* A dosimetric comparison of volumetric modulated arc therapy (VMAT) and non-coplanar intensity modulated radiotherapy (IMRT) for nasal cavity and paranasal sinus cancer. *Radiat Oncol.* **9,** 193 (2014).
17. Zhong-Hua, N. *et al.* Coplanar VMAT vs. noncoplanar VMAT in the treatment of sinonasal cancer. *Strahlenther Onkol.* **191,** 34–42 (2015).
18. Hodapp, N. The ICRU Report 83: prescribing, recording and reporting photon-beam intensity-modulated radiation therapy (IMRT). *Strahlenther Onkol.* **188,** 97–99 (2012).
19. Orlandi, E. *et al.* Radiotherapy for unresectable sinonasal cancers: dosimetric comparison of intensity modulated radiation therapy with coplanar and non-coplanar volumetric modulated arc therapy. *Radiother Oncol.* **113,** 260–266 (2014).
20. Paddick, I. A simple scoring ratio to index the conformity of radiosurgical treatment plans. Technical note. *J Neurosurg.* **93,** 219–222 (2000).
21. Vineberg, K. A. *et al.* Is uniform target dose possible in IMRT plans in the head and neck? *Int J Radiat Oncol Biol Phys.* **52,** 1159–1172 (2002).
22. Bhandare, N., Antonelli, P. J., Morris, C. G., Malayapa, R. S. & Mendenhall, W. M. Ototoxicity after radiotherapy for head and neck tumors. *Int J Radiat Oncol Biol Phys.* **67,** 469–479 (2007).
23. Sun, Y. *et al.* Radiation-induced temporal lobe injury after intensity modulated radiotherapy in nasopharyngeal carcinoma patients: a dose-volume-outcome analysis. *BMC Cancer.* **13,** 397 (2013).
24. Rodriguez-Caballero, A. *et al.* Cancer treatment-induced oral mucositis: a critical review. *Int J Oral Maxillofac Surg.* **41,** 225–238 (2012).
25. Ahmed, M., Hansen, V. N., Harrington, K. J. & Nutting, C. M. Reducing the risk of xerostomia and mandibular osteoradionecrosis: the potential benefits of intensity modulated radiotherapy in advanced oral cavity carcinoma. *Med Dosim.* **34,** 217–224 (2009).
26. Hsiung, C. Y. *et al.* Parotid-sparing intensity-modulated radiotherapy (IMRT) for nasopharyngeal carcinoma: preserved parotid function after IMRT on quantitative salivary scintigraphy, and comparison with historical data after conventional radiotherapy. *Int J Radiat Oncol Biol Phys.* **66,** 454–461 (2006).
27. Hall, E. J. & Wuu, C. S. Radiation-induced second cancers: the impact of 3D-CRT and IMRT. *Int J Radiat Oncol Biol Phys.* **56,** 83–88 (2003).
28. Broderick, M., Leech, M. & Coffey, M. Direct aperture optimization as a means of reducing the complexity of Intensity Modulated Radiation Therapy plans. *Radiat Oncol.* **4,** 8 (2009).
29. Jones, S. & Williams, M. Clinical evaluation of direct aperture optimization when applied to head-and-neck IMRT. *Med Dosim.* **33,** 86–92 (2008).
30. Dobler, B., Pohl, F., Bogner, L. & Koelbl, O. Comparison of direct machine parameter optimization versus fluence optimization with sequential sequencing in IMRT of hypopharyngeal carcinoma. *Radiat Oncol.* **2,** 33 (2007).
31. Verbakel, W. F. *et al.* Clinical application of a novel hybrid intensity-modulated radiotherapy technique for stage III lung cancer and dosimetric comparison with four other techniques. *Int J Radiat Oncol Biol Phys.* **83,** e297–303 (2012).

Author Contributions

J.Y.L., M.C. and B.-T.H. conceived and designed the experiments. J.Y.L., J.Y.Z. and Z.W.Z. performed the experiments. M.L., Y.K.L. and J.Z. analyzed the data. J.Y.L., J.Y.Z., M.L., Y.K.L. and J.Z. contributed materials/analysis tools. J.Y.L., J.Y.Z., M.L., Y.K.L., J.Z. and B.-T.H. wrote the paper.

Additional Information

Competing financial interests: The authors declare no competing financial interests.

How to cite this article: Lu, J.-Y. *et al.* A simple optimization approach for improving target dose homogeneity in intensity-modulated radiotherapy for sinonasal cancer. *Sci. Rep.* **5**, 15361; doi: 10.1038/srep15361 (2015).

This work is licensed under a Creative Commons Attribution 4.0 International License. The images or other third party material in this article are included in the article's Creative Commons license, unless indicated otherwise in the credit line; if the material is not included under the Creative Commons license, users will need to obtain permission from the license holder to reproduce the material. To view a copy of this license, visit http://creativecommons.org/licenses/by/4.0/